J Sol-Gel Sci Technol (2013) 68:204–212
DOI 10.1007/s10971-013-3152-0

ORIGINAL PAPER

Growth, structure and optical properties of tartaric acid-templated silica nanotubes by sol–gel method

Fei Gao · Yanhua Song · Ye Sheng · Chunming Lin · Qisheng Huo · Haifeng Zou

Received: 4 July 2013 / Accepted: 2 September 2013 / Published online: 24 September 2013

Abstract Photoluminescent nano material has been reported as an intriguing field during the past few decades. In this article, tartaric-templated silica nanotubes were conveniently synthesized by sol–gel method. X-ray diffraction analysis, scanning electron microscopy, transmission electron microscopy, fourier transform infrared spectra and photoluminescence spectra analysis were employed to characterize the growth, structure, morphology and optical property of the products. It is found that tartaric templates can form spindle/spherical-like aggregates composed of many sheets under static/stirring condition, which lead to the different shapes of silica nanotubes. Then the probable strategies for silica nanotubes templating with tartaric acid were described particularly. Hydrogen-bond interaction, supramolecular interaction and a competition of various effects may be the reasons of the nanotubes formation. Moreover, under ultraviolet light excitation, the silica nanotubes exhibited blue emission and luminescent intensity of the tubes prepared under the static condition is much stronger than the stirring ones, mostly because of more defect centers in the structures obtained under stirring condition.

Keywords Tartaric acid · Template · Silica nanotubes · Sol–gel · Photoluminescence

F. Gao · Y. Song · Y. Sheng · C. Lin · H. Zou (✉)
College of Chemistry, Jilin University, Changchun 130012, People's Republic of China
e-mail: haifengzou0431@gmail.com

Q. Huo
State Key Laboratory of Inorganic Synthesis and Preparative Chemistry, College of Chemistry, Jilin University, Changchun 130012, People's Republic of China

1 Introduction

Silica-based one-dimensional (1-D) nanostructured materials, such as wires [1], rods [2], tubes [3], helices [4], ribbons [5] and fibres [6], are gaining great attention because the Si–OH moieties on the surface of these nanomaterials make them easily functionalizable [7] using silane chemistry [8]. In particular, silica nanotubes raise special interest due to their optical, electrical, and mechanical properties [9]. It allows them to become potential candidates for application in many advanced fields such as catalysis [10], separation science [11], nanotechnology or drug delivery [12]. The photoluminescent property of silica nanostructured materials are expected to broaden potential applications which are often related to their size and morphology.

There are many methods to prepare silica nanotubes. The most frequently used method is template-directed sol–gel polycondensation of tetraethoxysilane (TEOS). In the past decade, silica nanotubes have been fabricated using organogels [13–15], hydrogels [16–19], carbon nanotubes [20], and porous alumina membranes as templates [21]. Nakamura and Matsui reported on the synthesis of silica materials with tubes and spheres using D,L-tartaric acid (TTA) and citric acid [22] as templates in addition of ammonia. The structures of ammonium-citrate crystals formed in quiescent conditions provide oriented attachable groups for patterning the tubular structure through specific interactions involving silanol groups. The method mentioned above was applied in numerous other SiO_2 syntheses [23, 24]. Some other inorganic salts were also employed as template agents for SiO_2 nanotubes synthesis, such as needle-like $CaCO_3$ NPs with TEOS as silica source [25]. TEOS is commonly used as the silica source because of its easily hydrolysis control, although other silica precursors

such as sodium silicate [26] can also be used. Luminescent silica nanotubes loaded with coumarion laser dye and with anthracene laser dye were also prepared by sol–gel co-condensation of functional dyes and TEOS in a cholesterol-based organogel system [27]. In any case, as a mild synthesis method for organic–inorganic functional materials, sol–gel process using organic templates can fabricate a large variety of optical and other materials easily.

The photoluminescence (PL) properties of silica have also been an important subject of research for a long time, PL from amorphous silica consists of bands in blue, red, green, and UV region [28]. Shen et al. [29] studied the red-light emission from siliceous MCM-41 with rapid thermal annealing (RTA) and observed a broad emission ranging from 580 to 670 nm. MCM-41 meso-porous nanotubes were also used to investigate the decay of blue–green luminescence at low temperature environment ranging from 50 to 300 K by Lee et al. [30]. Zhang et al. [31] reported macroscopic synthesis of silica nanotubes by the sol–gel template method and observed strong PL in both as-grown and annealed nanotube flakes, whose spectra have maxima at 486 nm (blue luminescence) and 539 nm (green–yellow light) for the as-grown and annealed samples, respectively. Subhasree Banerjee and Anindya Datta [28] used reverse micelle sol–gel method to prepare silica nanotubes and nanodisk, which exhibited blue photoluminescence. It was proposed that the intrinsic or extrinsic defects containing many centers in nature are responsible for these luminescence bands.

However, it is still not clarified particularly the formation of silica nanotubes and how they are interconnected with their optical properties. Inspired by the above discussion, we are interested in the details of the mechanism and dynamics properties of TTA-templated silica nanotubes formation. In this paper, we present the optimization of this process using a novel formation strategy that allows finely synthesizing different morphologies of the resulting nanometric silica structures. Hereafter, we discussed the photoluminescence of the SiO_2 nanotubes.

2 Experimental section

2.1 Materials and preparation

All the reagents such as D,L-TTA, absolute ethanol and ammonia were bought from Beijing Chemical Reagents Co., analytical grade and used without further purification. TEOS (99 %) was purchased from Internet Aladdin Reagent Database Inc. (Shanghai).

In the typical synthesis, 0.1 mmol TTA was dissolved in a mixture solution consisting 0.06 ml H_2O and 5 ml ethanol. TEOS (0.785 ml) was added into the above solution rapidly under static or stirring (magnetic stirring, 300 rpm) condition. The mixture was kept still for 30 min, and 2 ml NH_4OH (28 % NH_3 solution) was added after that. Finally, a white gel was obtained after staying for another 2 h. The gel was transferred into an oven which was sealed, and maintained at 110 °C for hours, followed by being thermally treated at 450 °C for 4 h, with a heating rate of 1 °C/min.

2.2 Characterization

The phase composition and phase structure of the as-synthesized products were examined by X-ray diffraction (XRD), using a Rigaku D/max-B II X-ray diffractometer with Cu Ka radiation. The morphologies, nanostructure and the composition analysis of the obtained silica nanotubes were characterized with a field emission scanning electron microscope (FESEM) (S-4800, Hitachi). Transmission electron microscopy (TEM) images were performed at a JEM-2000EX TEM (acceleration voltage of 200 kV). Fourier transform infrared (FT-IR) spectra were measured with a Perkin–Elmer 580B infrared spectrophotometer with the KBr pellet technique. The PL measurements were performed on Jobin–Yvon FluoroMax-4 luminescence spectrophotometer equipped with a 150 W xenon lamp as the excitation source. All the measurements were performed at room temperature.

3 Results and discussion

3.1 Synthetic process and morphology change

Transcription from the TTA templates to silica nanotubes was achieved under two different conditions in order to assess the role of stirring on the final morphology of the replicated objects. Figure 1 shows SEM and TEM images of silica nanotubes obtained under static and stirring conditions. The SEM images for the sample synthesized under static condition are presented in Fig. 1a, b. The sample is composed of bundles of nanotubes with length about several micrometers and the diameter about 350 nm. After calcinations at 450 °C, the samples maintain the morphology well, and the size has no obvious change. Figure 1c, d show the SEM images for the samples synthesized under stirring condition. We find that radial flower-like nanotubes are obtained [32], which possess rhomboid ends and shorter length than static condition. The average diameter and wall thickness of the tube are almost to 328 and 90 nm, respectively showed in the insets of Fig. 1b, d.

In general, the reaction environment has a great effect on the morphology of the final products. In the present

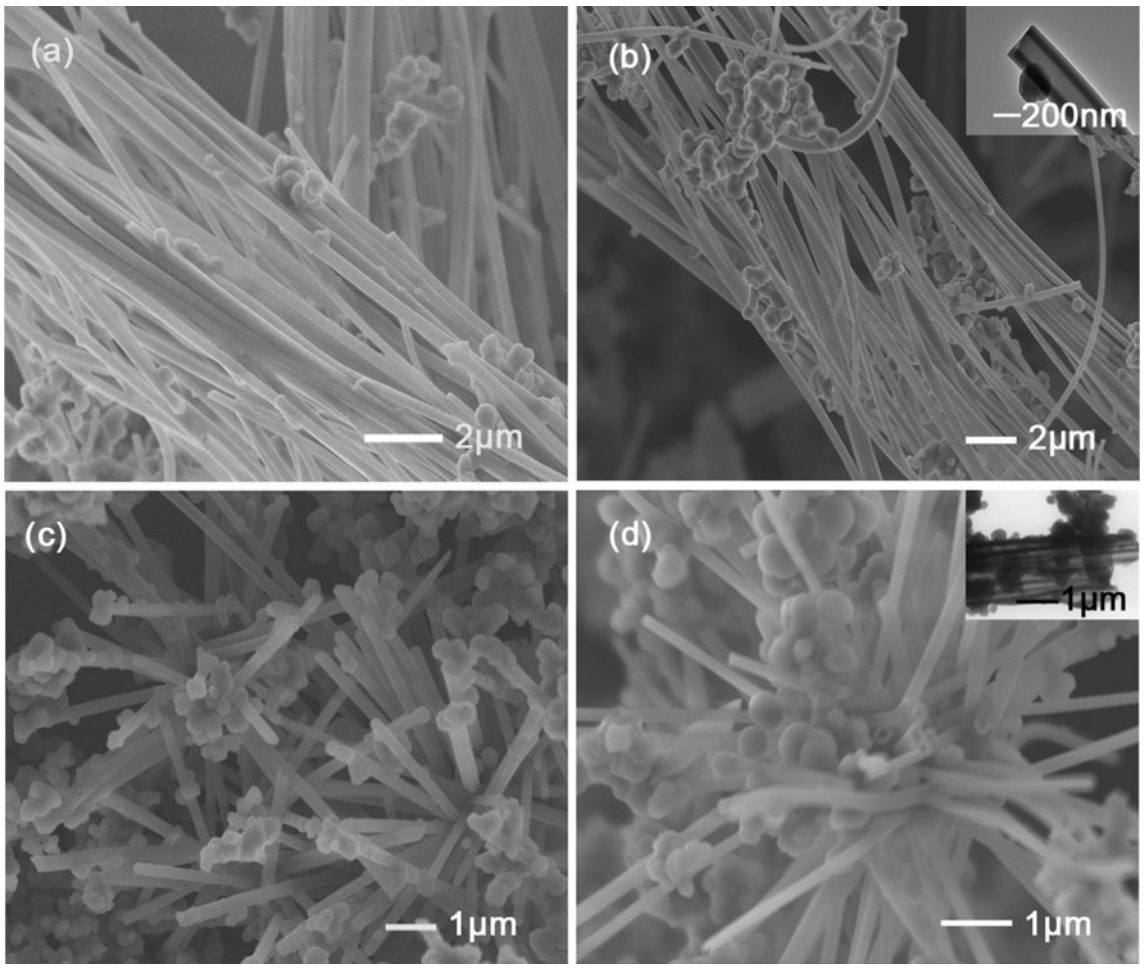

Fig. 1 SEM images of SiO_2 nanotubes: **a** pre-calcining under static condition, **b** post-calcining under static condition; **c** pre-calcining under stirring condition, **d** post-calcining under stirring condition. TEM images of SiO_2 nanotubes: *inset of* **b** post-calcining under static condition; *inset of* **d** post-calcining under stirring condition

system, the synthesis parameters, such as stirring or aging play an important role in controlling the morphology of the SiO_2 nanotubes. Firstly, we investigate the formation process of silica nanotubes. Then the influences of stirring and aging on the morphology evolutions of the SiO_2 nanotubes are discussed.

There are two stages in the whole process of silica tubes templated by TTA, in which NH_4OH addition can be a demarcation point.

TEOS can not hydrolysis or partial hydrolysis with the time prior to ammonium hydroxide addition. Without ammonium hydroxide, only the aggregations of TTA are changed with the time. Under the absolute static condition, we observe spindle TTA molecules form in the first 5 min (Fig. 2a). The aggregations composed of many sheets are observed as time goes by. Some pre-split sheets exhibit well defined shape in Fig. 2b. In the last period before NH_4OH addition, hundreds of flower-like aggregated materials are obvious, with the different amounts of "petals" (Fig. 2c). Figure 2d, e show the sample obtained after adding NH_4OH at different point-in-times. First, TEOS hydrolyzes rapidly and deposits on the surface of the templates, which are totally packed (Fig. 2d). Then the micro tubes with smooth surface are observed by a slow aggregation process. Interestingly, several layered structure form on one micro tube, which seems that thinner tubes are going to come out, as shown in Fig. 2e. Two hours after adding NH_4OH, a large number of nanotubes are obtained (Fig. 2f), with uniform length and outer diameter, about hundreds of microns and 350 nm, respectively.

In contrast, when the TEOS was introduced under stirring condition, the nanotubes with flower-like structure are observed. And then we study the morphology of the templates. At first, when stirring for 5–10 min after TEOS addition, we find bulk aggregations 5 min later (Fig. 3a). As Fig. 3b shows, with the self-assembly of TTA templates proceeds, the spherical aggregations are observed and the sheets on them split and shrink. The helical deformation begins at the central of the spherical aggregations. Meanwhile, the spherical particles emerge increasingly, different

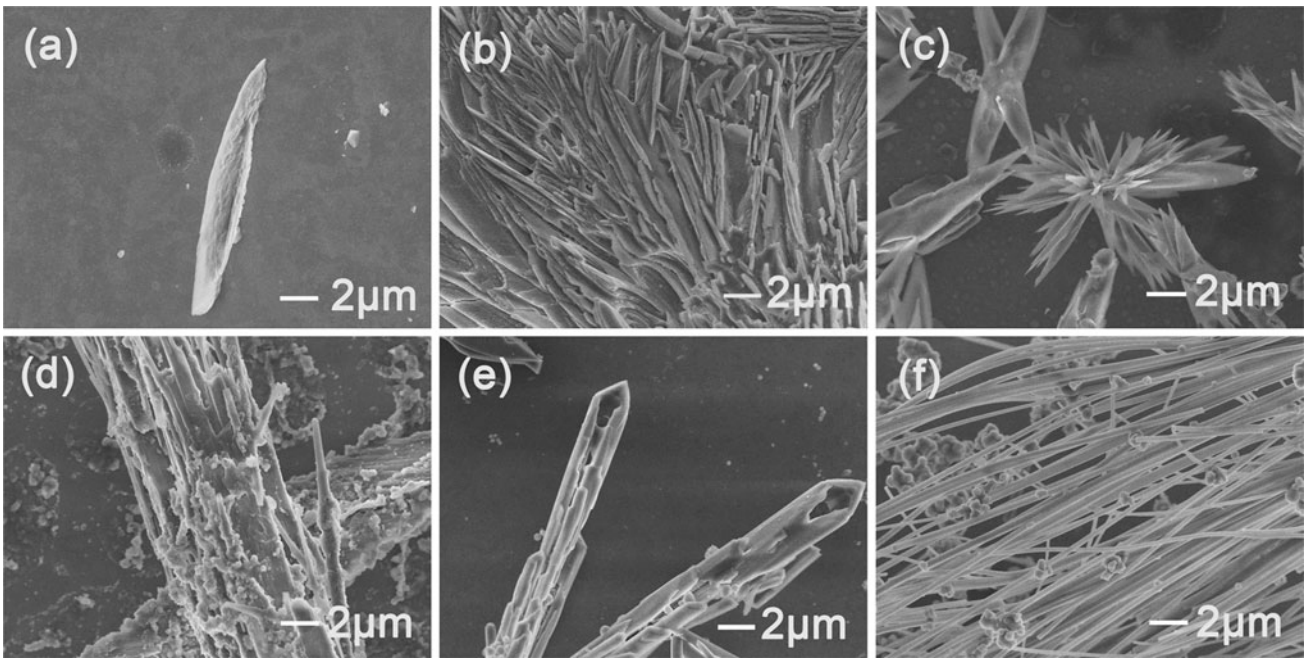

Fig. 2 SEM images of the samples synthesized at different stage under static condition **a** 5 min, **b** 10 min, **c** 30 min (before NH_4OH addition); **d** 0 min, **e** 30 min, **f** 2 h (after NH_4OH addition)

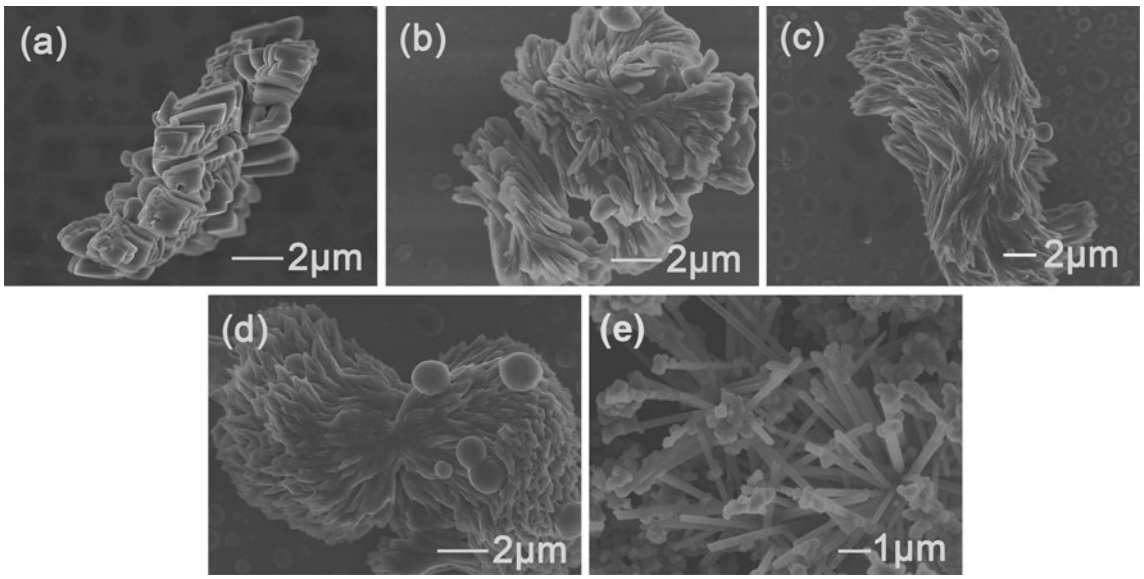

Fig. 3 SEM images of the samples synthesized at different stage under stirring condition **a** 5 min, **b** 10 min, **c** 20 min, **d** 30 min (before NH_4OH addition); **e** 2 h (after NH_4OH addition)

from the static condition (Fig. 3c, d). We obtain radial flower-like nanotubes after adding NH_4OH, which have obvious distinction with the previous products on morphology, shown in Fig. 3e.

It follows that stirring and aging are two crucial influencing factors to the formation of silica nanotubes. They have different mechanism of action in the chemical process of our products.

Stirring may have two effects: morphology influence of the assembled template or TEOS diffusion to the reaction system. The SEM photographs reveal that only the former work. On the one hand, shearing force due to stirring makes both ends of TTA-spherical aggregations rotate inversely based on the same vertical axis, and which bring about the generation of spherical TTA. Meanwhile, the spherical particles are obtained increasingly over time on

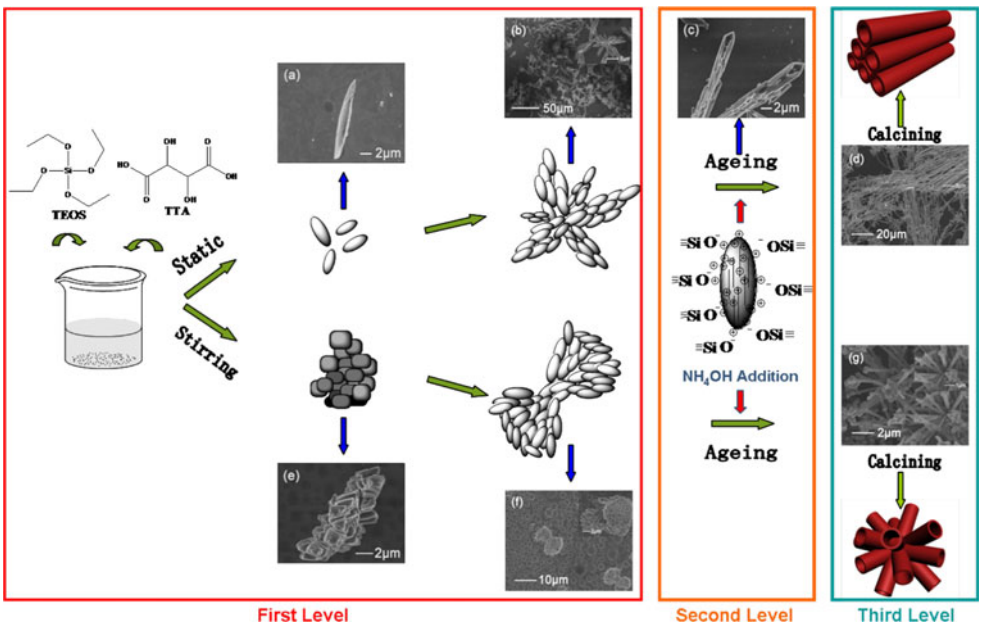

Scheme 1 Scheme illustration for the formation process of clump-shaped and radial flower-like SiO_2 nanotubes SEM images of the samples synthesized at different stage under static condition: **a** 5 min, **b** 30 min (before NH_4OH addition); **c** 30 min **d** 2 h (after NH_4OH addition). SEM images of the samples synthesized at different stage under stirring condition: **e** 5 min, **f** 30 min (before NH_4OH addition); **g** 2 h (after NH_4OH addition)

the other. In addition, we believe the nucleus are not scattered arising from the latter effect in view of our experimental phenomenon.

Aging effects is one of the post-templating variables affecting the shape, size, and yield of the silica objects strongly. Once TEOS has enough time (30 min) to self-assemble around the template before ammonium hydroxide addition, gelation after base addition will make the TEOS hydrolyze completely onto the template with ideal tube. Interestingly, if extended times are used before base addition, the formed silica appears to be particles. This presumably because the TTA aggregates that initially forms before base addition has re-dissolved, and then there are relatively few templates for partial hydrolyzed TEOS to attach. This result reveals the importance of obtaining appropriate aging effects in forming the silica structure [33].

Also, we varied the TTA dosage and the temperature of both gel formation and silica transcription. There are no obvious effects about the morphology of the tubes like stirring or aging does.

3.2 Main strategies for silica nanotubes templating with TTA

The mechanism of tubular growth of silica nanotubes is discussed.

3.2.1 First step (I)

The intermolecular hydrogen-bonding structure is the combination mode of TTA molecules. In our opinion, the tartaric groups are probably linked to each other by H-bonds between carboxylic and hydroxyl groups to form a molecular ensemble, which assemble the spindle aggregates on a macro level under the condition of the partial hydrolysis of TEOS. Moreover, these TTA aggregates are the templates for TEOS because they have formed before NH_4OH addition and affect the morphology of the tubes ultimately. As the Scheme 1 shows, spherical aggregations of TTA lead to the formation of the flower-like nanotubes.

After that, the templates transcription takes place through a cooperative co-assembly process (the in situ forming TTA fibrils direct the growth of spindle silica, and vice versa, the condensing TEOS affects the way the TTA molecules self-assemble). Herein, nanofibrous hybrid composite materials can be obtained, which consist of TTA coated with the partially condensed TEOS. These latter ones can locate onto the external surfaces of the spindle nanofibrils.

3.2.2 Second step (II)

Supramolecular interactions between TTA molecules and TEOS play a decisive role in efficient transcription from the templates to products. In general, electrostatic interaction can be responsible for it. After ammonium hydroxide addition, the oligomeric silica species are adsorbed onto the cationic fibrils and the polymerization further proceeds along these fibrils. In this process ammonium groups are inserted among TTA molecules by H-bonds along with the addition at first. Then the structures of ammonium-tartrate aggregates formed in quiescent conditions provide oriented attachable groups for patterning the tubular structure through specific interaction involving silanol groups. That is, externally added positive charges coming from ammonium ion may be incorporated

with TTA aggregates through complexation, and therefore these aggregates enabled the transcription into silica in the presence of metalloid salts (Tartrate·$NH_4^+\cdots^-$O–Si≡).

3.2.3 Third step (III)

When the supramolecular interactions have been established among TTA templates, silica precursors and solvent molecules, the silica condensation kinetics are initiated simultaneously. At this step, a competition occurs between the condensation of TEOS in the solvent and that onto the surface of templates, which mainly owing to solution and surface mechanism respectively. In order to make the transcription of silica efficiently, the surface mechanism must work dominantly comparing with the solution mechanism, and this depends simultaneously on the strength of such as supramolecular interactions, sol–gel condensation kinetics, and solvent or surface effects.

Specifically, when silica polymerization occurs preferentially near the surfaces of the templates (diameter about several micrometers), silica can not only grow onto the templates but also into their inner gaps, causing the formation of microfibrous objects. Consequently, the sol–gel polymerization occurs on and in the microfibers, leading to the separation of the microfibers and the fabrication of silica nanotubes. In contrast, if shearing force is introduced, many non-templated species which will evolve into the spherical particles emerge. At the same time of these

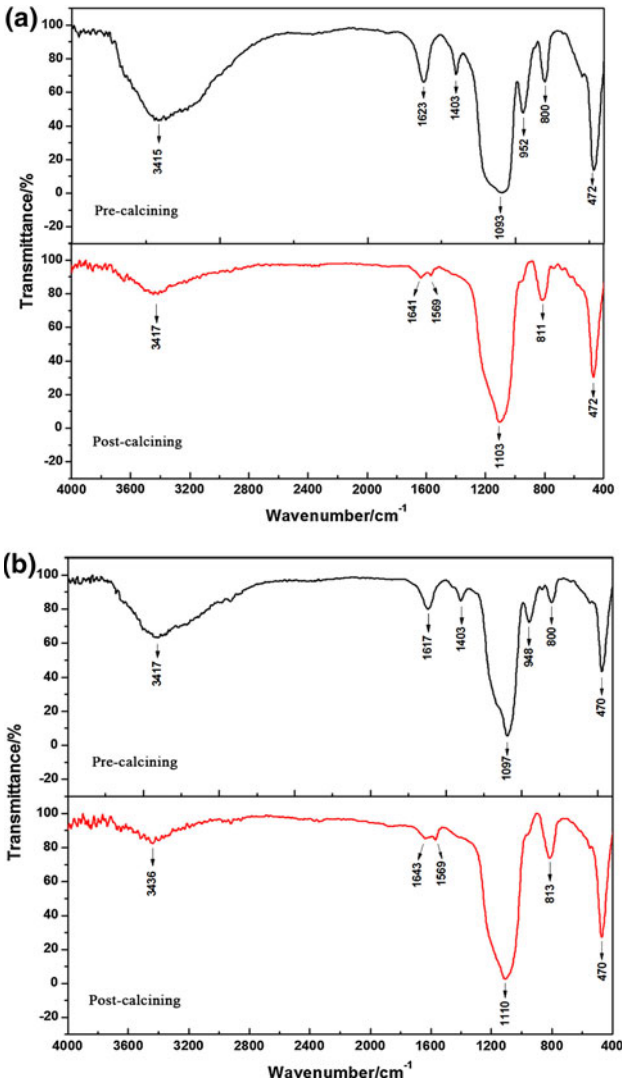

Fig. 4 FT-IR spectra of SiO_2 nanotubes: **a** under static condition; **b** under stirring condition

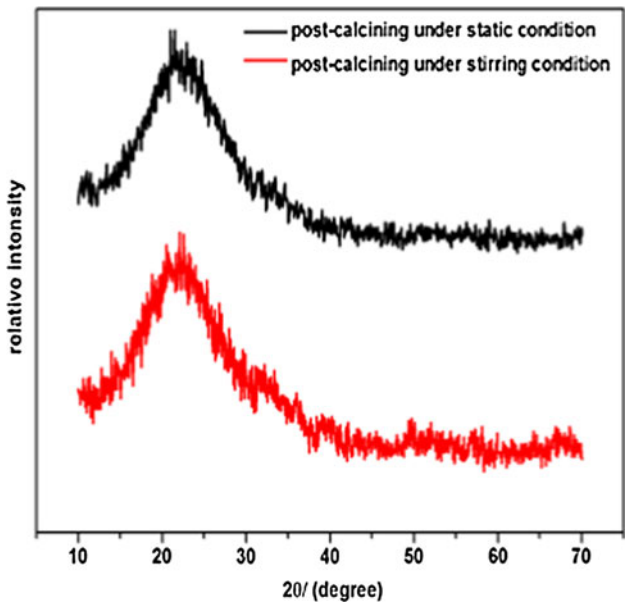

Fig. 5 XRD patterns of SiO_2 nanotubes prepared by different conditions

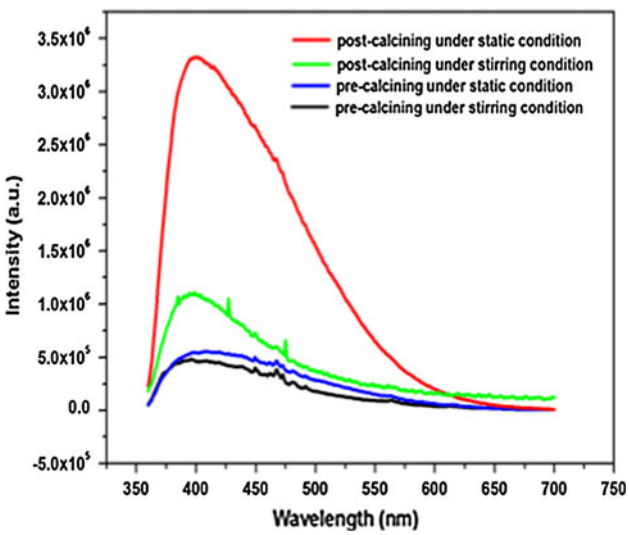

Fig. 6 PL spectra of SiO_2 nanotubes prepared by different conditions

Scheme 2 Scheme of hydrolysis and condensation model of TEOS

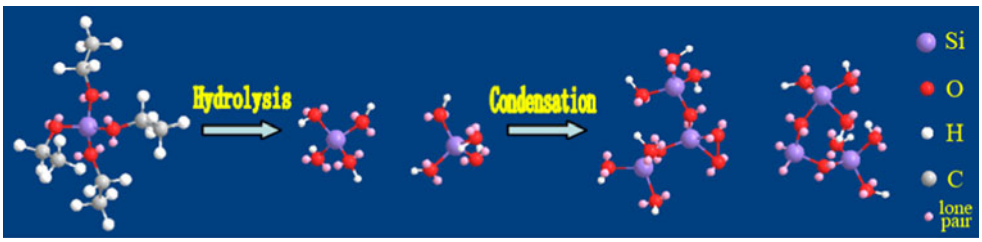

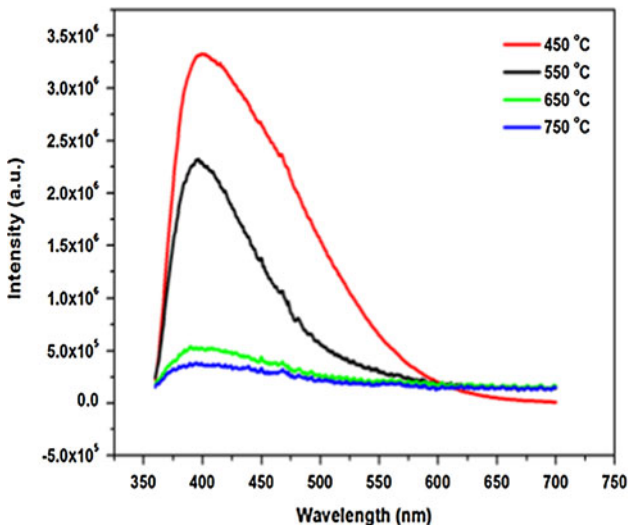

Fig. 7 PL spectra of SiO_2 nanotubes prepared under static condition at different calcining temperatures

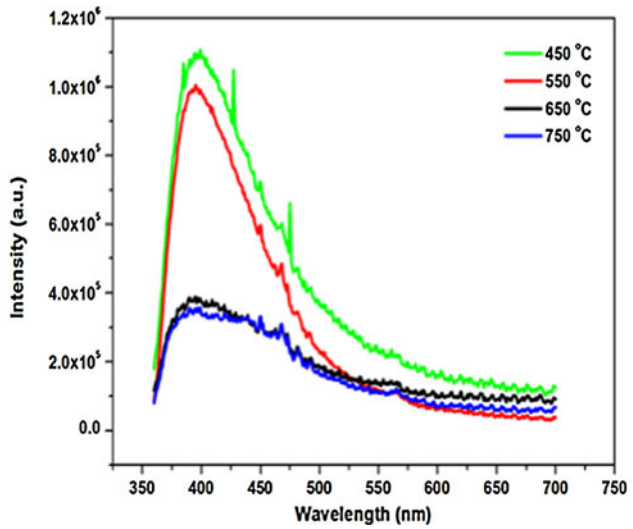

Fig. 8 PL spectra of SiO_2 nanotubes prepared under stirring at different calcining temperatures

processes, the sufficient objects may entrap the solvent molecules in Si–O–Si network and then gels have formed. Finally, the templates are removed by calcination treatment and the pure silica nanotubes are obtained.

3.3 Properties of silica nanotubes

3.3.1 FT-IR spectra analysis

Since Si–OH in silica gels dose not condense into Si–O–Si network entirely, the number of –OH groups will be more before calcining. This is clear from the FT-IR spectra of silica nanotubes under static and stirring condition (Fig. 4). The Si–OH vibration mode is strongly present in silica nanotubes under both static (at 952 cm^{-1}, Fig. 4a) and stirring condition (at 948 cm^{-1}, Fig. 4b) before calcining. The broad bands between 2,800 and 3,200 cm^{-1} show that, in addition to the chain ending –OH groups, the free water molecules are also high in both silica products before thermal treatment where as very weak after.

3.3.2 Structures

Figure 5 shows XRD spectra of silica nanotubes obtained under stirring and static condition after calcination treatment. The broad peaking at $2\theta = 22.5°$ can be assigned to the characteristic diffraction for the amorphous silica. The diffracted intensity decays gradually and fluctuates slightly soon afterward. This is in good agreement with the performance that amorphous silica materials generally have.

3.3.3 Luminescence properties

Figure 6 displays PL spectra for the silica nanotubes obtained under stirring and static condition. At 330 nm excitation, all PL curves have a blue band region. In each case, only one peak with no shoulder can be observed. This is largely in line with the observation for the silica gel [28]. That can be ascribed to a particular kind of defect center, with some contribution from surface-associated defects. Uchino et al. [34] have proposed an model that two geminal silanol groups co-condense to yield a metastable defect pair consisting of dioxasilirane, $=Si(O_2)$, and silylene, =Si:, centers (Scheme 2), which can account for the underlying experimental features related to the blue-PL band. It is reported that the radiative transitions are strongly quenched by the high frequency vibrations of –OH groups [35]. This quenching by –OH groups also results in decreased luminescence in silica nanotubes, which can explain the PL intensity of nanotubes after calcining are stronger than

before under both static and stirring condition. Interestingly, the SiO_2 tubes under stirring condition show weaker PL intensity. That may be the result of more spherical particles emerging with TTA aggregations because of shearing force. Comparing to particles, nanotube has more defects on or in its outer and inner surface. That is why the products prepared under static condition who own more tubes have better optical property.

Meanwhile, the evidence reflecting in the PL spectra of SiO_2 nanotubes at different calcining temperatures indicate that the PL intensity reduce gradually as temperature rise, no matter what the condition (Figs. 7, 8). It is probably that higher temperatures (>450 °C) will destroy the metastable defect centers aforementioned, which even lead to sintering and structure collapse. In a similar way, we can find the curves at 450 °C showed in Figs. 7 and 8 have relatively better distribution than the higher temperatures.

4 Conclusions

In conclusion, silica nanotubes are fabricated through supramolecular interactions among the ammonium tartrate and the condensing tetraethoxysilane, which are conveniently prepared through sol–gel transcription of TEOS by using TTA as templates. It is found that tartaric molecules can form microaggregations made of many fibrils before NH_4OH addition, probably through H-bonding interactions. It makes tartaric serve as the framework of the templates rather than ammonium tartrate. A co-assembly mechanism is put forward to describe the formation process of silica nanotubes. Furthermore, the morphology of silica nanotubes can be varied by providing shearing force (stirring), which can affect the formation of tartaric and then the tubes as flower-like aggregates are obtained. The photoluminescent of blue emission of silica nanotubes are achieved. The luminescent intensity of the tubes prepared under the static condition is much stronger than the stirring ones, mostly because of more defect centers in their structures. In addition, microstructure may also change greatly with variation of calcining temperature. The photoluminescent silica nanotubes are expected to broaden potential applications in optics, sensing, and biomedical engineering.

Acknowledgments This work was supported by the National Natural Science Foundation of China (Grant No. 51272085) and the Opening Research Funds Projects of the State Key Laboratory of Inorganic Synthesis and Preparative Chemistry and College of Chemistry, Jilin University (2010–05).

References

1. Ying JY (1997) Preface to the special issue: sol–gel derived materials. Chem Mater 9(11):2247–2248. doi:10.1021/cm970999y
2. Lee KG, Wi R, Imran M, Park TJ, Lee J, Lee SY, Kim DH (2010) Functionalization effects of single-walled carbon nanotubes as templates for the synthesis of silica nanorods and study of growing mechanism of silica. ACS Nano 4(7): 3933–3942
3. Nakamura H, Matsui Y (1995) Silica gel nanotubes obtained by the sol–gel method. J Am Chem Soc 117(9):2651–2652
4. Delclos T, Aimé C, Pouget E, Brizard A, Huc I, Delville M-H, Oda R (2008) Individualized silica nanohelices and nanotubes: tuning inorganic nanostructures using lipidic self-assemblies. Nano Lett 8(7):1929–1935
5. Chen Y, Wang S, Liu X, Li Y, Li B, Yang Y (2010) Formation of left-handed double twisted silica nanoribbons. Chin J Chem 28(10):1941–1945
6. Geltmeyer J, Van der Schueren L, Goethals F, De Buysser K, De Clerck K (2013) Optimum sol viscosity for stable electro spinning of silica nano fibres. J Solgel Sci Technol 67(1):188–195. doi:10.1007/s10971-013-3066-x
7. Su X, Zhao J, Zhao X, Guo Y, Zhu Y, Wang Z (2008) A facile synthesis of Cu_2O/SiO_2 and Cu/SiO_2 core–shell octahedral nanocomposites. Nanotechnology 19(36):365610
8. Han WS, Kang Y, Lee SJ, Lee H, Do Y, Lee Y-A, Jung JH (2005) Fabrication of color-tunable luminescent silica nanotubes loaded with functional dyes using a sol–gel co condensation method. J Phys Chem B 109(44):20661–20664
9. García-Calzón JA, Díaz-García ME (2012) Synthesis and analytical potential of silica nanotubes. TrAC, Trends Anal Chem 35:27–38. doi:10.1016/j.trac.2012.01.003
10. Dong W, Zhao H, Li C, Mei J, Chen B, Tang W, Shi Z, Feng S (2011) Hetero-nanostructure of silver nanoparticles on MOx (M = Mo, Ti and Si) and their applications. Sci China Chem 54(6):865–875
11. Mitchell DT, Lee SB, Trofin L, Li N, Nevanen TK, Söderlund H, Martin CR (2002) Smart nanotubes for bioseparations and biocatalysis. J Am Chem Soc 124(40):11864–11865
12. Chen CC, Liu YC, Wu CH, Yeh CC, Su MT, Wu YC (2005) Preparation of fluorescent silica nanotubes and their application in gene delivery. Adv Mater 17(4):404–407
13. Clavier GM, Pozzo JL, Bouas-Laurent H, Liere C, Roux C, Sanchez C (2000) Organogelators for making porous sol-gel derived silica at two different length scales. J Mater Chem 10(7):1725–1730. doi:10.1039/B000525H
14. Huang X, Weiss RG (2006) Silica structures templated on fibers of tetraalkylphosphonium salt gelators in organogels. Langmuir 22(20):8542–8552
15. Xue P, Lu R, Li D, Jin M, Bao C, Zhao Y, Wang Z (2004) Rearrangement of the aggregation of the gelator during sol–gel transcription of a dimeric cholesterol-based viologen derivative into fibrous silica. Chem Mater 16(19):3702–3707
16. Lin Y, Qiao Y, Gao C, Tang P, Liu Y, Li Z, Yan Y, Huang J (2010) Tunable one-dimensional helical nanostructures: from supramolecular self-assemblies to silica nanomaterials. Chem Mater 22(24):6711–6717. doi:10.1021/cm102181e
17. Gundiah G, Mukhopadhyay S, Tumkurkar UG, Govindaraj A, Maitra U, Rao C (2003) Hydrogel route to nanotubes of metal oxides and sulfates. J Mater Chem 13(9):2118–2122
18. Yuwono VM, Hartgerink JD (2007) Peptide amphiphile nanofibers template and catalyze silica nanotube formation. Langmuir 23(9):5033–5038
19. Dickerson MB, Sandhage KH, Naik RR (2008) Protein-and peptide-directed syntheses of inorganic materials. Chem Rev 108(11):4935
20. Caruso RA, Antonietti M (2001) Sol–gel nanocoating: an approach to the preparation of structured materials. Chem Mater 13(10):3272–3282. doi:10.1021/cm001257z

21. Fan R, Wu Y, Li D, Yue M, Majumdar A, Yang P (2003) Fabrication of silica nanotube arrays from vertical silicon nanowire templates. J Am Chem Soc 125(18):5254–5255
22. Nakamura H, Matsui Y (1995) The preparation of novel silica gel hollow tubes. Adv Mater 7(10):871–872
23. Lim A, Schueneman G, Novak B (1999) Solid state NMR of SiO_2 nanotube coated ammonium tartrate crystal. Solid State Commun 110(6):333–338
24. Anastasescu C, Zaharescu M, Balint I (2009) Unexpected photocatalytic activity of simple and platinum modified tubular SiO_2 for the oxidation of oxalic acid to CO_2. Catal Lett 132(1–2):81–86. doi:10.1007/s10562-009-0066-0
25. Xiao Q-G, Tao X, Chen J-F (2007) Silica nanotubes based on needle-like calcium carbonate: fabrication and immobilization for glucose oxidase. Ind Eng Chem Res 46(2):459–463
26. Khoabane K, Mokoena EM, Coville NJ (2005) Synthesis and study of ammonium oxalate sol–gel templated silica gels. Microporous Mesoporous Mater 83(1–3):67–75. doi:10.1016/j.micromeso.2005.04.002
27. Anastasescu C, Anastasescu M, Teodorescu VS, Gartner M, Zaharescu M (2010) SiO_2 nanospheres and tubes obtained by sol–gel method. J Non Cryst Solids 356(44–49):2634–2640. doi:10.1016/j.jnoncrysol.2010.03.038
28. Banerjee S, Datta A (2010) Photoluminescent silica nanotubes and nanodisks prepared by the reverse micelle sol–gel method. Langmuir 26(2):1172–1176. doi:10.1021/la902265e
29. Shen J, Chen P, Lee Y, Cheng C (2002) Red-light emission in MCM-41 meso-porous nanotubes. Solid State Commun 122(1):65–68
30. Lee YC, Liu YL, Wang CK, Shen JL, Cheng PW, Cheng CF, Ko CH, Lin TY (2005) Decay dynamics of blue–green luminescence in meso-porous MCM-41 nanotubes. J Lumin 113(3–4):258–264. doi:10.1016/j.jlumin.2004.10.026
31. Zhang M, Ciocan E, Bando Y, Wada K, Cheng LL, Pirouz P (2002) Bright visible photoluminescence from silica nanotube flakes prepared by the sol–gel template method. Appl Phys Lett 80(3):491. doi:10.1063/1.1434309
32. Liu H, Huang J, Li X, Liu J, Zhang Y (2012) One-step hydrothermal synthesis of flower-like SnO_2/carbon nanotubes composite and its electrochemical properties. J Solgel Sci Technol 63(3):569–572
33. Mokoena E, Datye A, Coville N (2003) A systematic study of the use of DL-Tartaric acid in the synthesis of silica materials obtained by the sol–gel method. J Solgel Sci Technol 28(3):307–317. doi:10.1023/A:1027418230211
34. Uchino T, Kurumoto N, Sagawa N (2006) Structure and formation mechanism of blue-light-emitting centers in silicon and silica-based nanostructured materials. Phys Rev B 73(23). doi: 10.1103/PhysRevB.73.233203
35. Thomas V, Jose G, Jose G, Biju P, Rajagopal S, Unnikrishnan N (2005) Structural evolution and fluorescence properties of Dy^{3+}: silica matrix. J Solgel Sci Technol 33(3):269–274